NASA TECHNICAL NOTE

NASA TN D-4226

NASA TN D-4226
c.1

NASA TN D-4226

A STEREOGRAPHIC REPRESENTATION OF KNOOP HARDNESS ANISOTROPY

by M. Garfinkle and R. G. Garlick

Lewis Research Center
Cleveland, Ohio

NATIONAL AERONAUTICS AND SPACE ADMINISTRATION • WASHINGTON, D. C. • NOVEMBER 1967

A STEREOGRAPHIC REPRESENTATION OF KNOOP HARDNESS ANISOTROPY

By M. Garfinkle and R. G. Garlick

Lewis Research Center
Cleveland, Ohio

NATIONAL AERONAUTICS AND SPACE ADMINISTRATION

For sale by the Clearinghouse for Federal Scientific and Technical Information
Springfield, Virginia 22151 – CFSTI price $3.00

A STEREOGRAPHIC REPRESENTATION OF KNOOP HARDNESS ANISOTROPY

by M. Garfinkle and R. G. Garlick

Lewis Research Center

SUMMARY

During the course of an investigation of the hardness anisotropy of several body-centered-cubic (BCC) metal crystals, it became evident that the variation of Knoop hardness with crystallographic orientation was dependent essentially on the direction of the long axis of the indentor alone, and not on the plane of indentation. The study was extended to include a face-centered-cubic (FCC) and a close-packed-hexagonal (CPH) metal and an ionic crystal to determine the generalities of this observation. For cubic crystals, this observation was valid; for the CPH structure, however, the planes of identification did have some effect on the hardness anisotropy, although this was not nearly as significant as the direction of indentation. Because the direction of indentation is the only significant crystallographic parameter necessary to describe the hardness anisotropy, it is possible to represent the anisotropy of single crystals on the standard stereographic triangle.

INTRODUCTION

The commonly observed (refs. 1 and 2) periodic variation of indentation hardness with crystallographic direction on the high-symmetry planes of various single crystals has been inadequately related to the physical or mechanical properties of the crystals examined. In fact, the hardness anisotropy curves for the various planes of a particular metal crystal (as is illustrated in fig. 1) are uncorrelated and appear in the literature (refs. 3 and 4) as unrelated observations. Attempts to correlate hardness anisotropy curves with specific physical properties can be generally divided into either mechanistic or nonmechanistic approaches.

A nonmechanistic approach would be to devise a mathematical expression that could

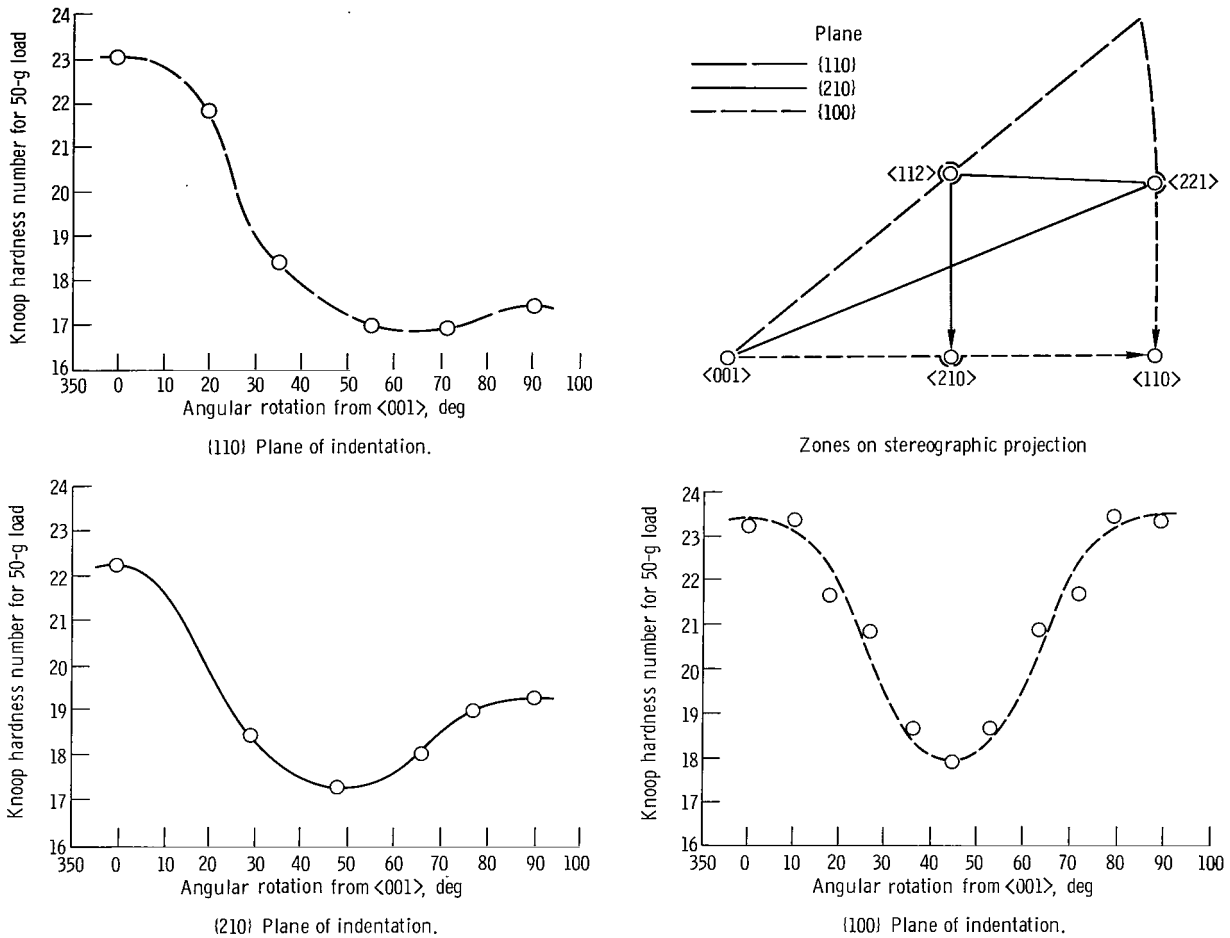

Figure 1. - Variation of Knoop hardness on three planes of aluminum and representation of these planes on stereographic projection.

describe the various hardness anisotropy curves. Such a relation could then be compared with the known anisotropy of various physical properties to determine which contribute to the observed hardness anisotropy. No such mathematical expression has been found in the literature.

A mechanistic approach would be concerned with the actual mode of deformation resulting from indentation in relation to some factor that is dependent on crystal anisotropy, such as resolved shear stress. An analysis by Daniels and Dunn (ref. 5) is apparently the only attempted comprehensive explanation of the hardness anisotropy of single crystals. However, inconsistencies were found in their analysis. These are considered in the DISCUSSION section.

In light of the unsuccessful attempts to analyze hardness anisotropy curves in terms of physical or mechanical properties, the anisotropy curves from our investigation of several crystals were examined simply to determine whether any features were common among the curves that might permit some degree of correlation.

EXPERIMENTAL PROCEDURE

The metal crystals examined in this analysis of hardness anisotropy represent the three common crystal structures of metals. Tungsten, tungsten - 3.2-percent rhenium (W-3.2Re), and niobium single crystals, prepared by the vacuum floating-zone process, are body-centered cubic (BCC). Aluminum, which was grown by the horizontal-crucible zone-melting process, is face-centered cubic (FCC). The close-packed hexagonal structure (CPH) is represented by titanium, prepared by the strain-anneal process. Lithium fluoride (LiF), a FCC nonmetal, grown as a boule from the melt, was also included to determine whether this analysis would apply to an ionic crystal. None of the crystals had impurity levels greater than 0.1 percent.

The cubic-crystal metals were sectioned by a spark-cutter to expose the {100}, {110}, and {210} planes. The $\{\bar{1}100\}$, $\{\bar{1}2\bar{1}0\}$, $\{\bar{5}7\bar{2}0\}$, and (0001)[1] planes were exposed on the HCP titanium crystal. The $\{\bar{5}7\bar{2}0\}$ prismatic plane is 14° from the $\{\bar{1}2\bar{1}0\}$. The individual crystals of the various materials were then mounted in either phenolic resin or cold-setting plastic, and subsequently chemically or electrolytically polished to remove the worked surface layer. The LiF was mechanically ground and polished. All planes and directions are within 3° of those indicated.

All hardness determinations were made with a microhardness tester using a Knoop indentor. This indentor consists of a mounted inverted diamond pyramid that would, if elastic recovery were absent, produce an elongated impression with a length that is about 7 times its width and 30 times its depth (ref. 6). Only the long axis of the impression d is significant in computing the Knoop hardness number (KHN). Because the only significant measurement is in a single direction, this hardness test is well suited to a hardness anisotropy study. The hardness impressions were made with the long axis of the indentor alined with predetermined crystallographic directions on the planes of interest.

The KHN has the same units as stress, and is equal to $14.32\ L/d^2$ where L is the applied load and d is the length of the impression. The load for each material tested is listed in table I, and was applied for 33 seconds for each impression. Cracks were not observed to be associated with any of the impressions. Hardness values were averaged from at least 10 impressions, and are tabulated in table I with their mean deviations. The mean deviation is a measure of the data scatter about the mean hardness value. The magnitude of the mean deviation is a function of bulk effects, such as material inhomogeneity and surface effects, such as surface flatness.

Hardness impressions were made in various directions on the {100}, {110}, and {210} planes of the cubic crystals and on the (0001), $\{\bar{1}100\}$, $\{\bar{1}2\bar{1}0\}$, and $\{\bar{5}7\bar{2}0\}$ planes of the hexagonal crystal.

[1]The conventional representation of indices for general planes and directions are {hkl} and ⟨hkl⟩, respectively, and the representation for specific planes and directions are (hkl) and [hkl], respectively.

TABLE I. - KNOOP HARDNESS ANISOTROPY DATA FOR SEVERAL CUBIC CRYSTALS

System		Aluminum		Lithium fluoride		Tungsten		Tungsten-3.2 percent rhenium		Niobium	
Direction	Plane	Knoop hardness number									
		25-g load	Mean value	300-g load	Mean value	1000-g load	Mean value	1000-g load	Mean value	100-g load	Mean valve
⟨100⟩	{100}	23.1 ± 1.1	22.6	87.5 ± 0.8	87.0	399 ± 4	404	362 ± 3	375	79.1 ± 0.9	80.9
	{110}	22.6 ± 0.5		89.2 ± 1.2		408 ± 6		398 ± 6		83.5 ± 0.7	
	{210}	22.1 ± 0.3		84.4 ± 0.8		405 ± 7		366 ± 4		81.0 ± 1.5	
⟨110⟩	{100}	18.2 ± 0.5	17.8	94.1 ± 1.5	93.3	342 ± 4	337	279 ± 5	282	56.7 ± 1.5	58.4
	{110}	17.3 ± 0.4		92.5 ± 0.4		332 ± 7		284 ± 5		60.1 ± 0.6	
⟨210⟩	{100}	20.6 ± 0.8	19.9	95.6 ± 1.0	95.8	359 ± 4	359	304 ± 5	309	63.4 ± 1.2	64.7
	{210}	19.1 ± 0.3		95.9 ± 0.6		359 ± 7		314 ± 2		66.0 ± 0.5	
⟨211⟩	{110}	18.4 ± 0.6	18.3	96.5 ± 0.9	96.0	351 ± 15	341	299 ± 4	295	62.7 ± 4.4	62.8
	{210}	18.1 ± 0.5		95.4 ± 0.5		331 ± 6		291 ± 4		62.9 ± 0.7	
⟨221⟩	{110}	16.7 ± 0.4	17.1	94.1 ± 0.6	95.9	336 ± 3	334	286 ± 3	284	64.0 ± 0.8	62.9
	{210}	17.5 ± 0.5		97.6 ± 0.3		331 ± 3		282 ± 4		61.7 ± 0.8	
⟨421⟩	{210}	18.3 ± 0.5	18.6	94.9 ± 1.1	94.3	341 ± 7	348	318 ± 5	311	63.0 ± 0.7	62.3
	{210}	18.8 ± 0.4		95.6 ± 0.9		355 ± 7		303 ± 2		61.5 ± 0.7	

RESULTS

Hardness anisotropy curves were prepared from the experimental data for each plane of each crystal on which hardness impressions were made. The curves for aluminum are illustrated in figure 1. A detailed examination of these curves shows that the hardness values are very similar in the same crystallographic directions. For example, on the {100}, {110}, and {210} planes, the hardness values in the ⟨100⟩ direction are 23.1, 22.6, and 22.1, respectively. If this observation is correct, that hardness anisotropy is primarily a function of the direction of indentation alone and is not significantly dependent on the plane of indentation, then this is the factor that relates the hardness anisotropy curves for different planes.

To determine if this observation is generally valid for cubic crystals, the hardness values and their mean deviations for the 5 cubic materials were tabulated (table I) to permit comparison of the hardnesses in the same direction on the various planes. The differences in the hardness values in the same direction may be attributed to errors in alining the indentor in the directions indicated, as well as minor planar effects. This tabulation indicates that hardness anisotropy is primarily a function of direction of indentation.

With the hardness anisotropies dependent on only one geometric parameter the crystallographic direction of indentation, it is possible to represent the hardness anisotropy of a cubic crystal on a representative triangular portion of a standard stereographic projection. A stereographic triangle can represent the hardness in all directions of a single crystal, and thus, can readily permit a comparison of the hardness in different directions.

On the stereographic triangle, the planes of indentation appear as zones and the directions of indentation as points. Figure 1 illustrates the position of the {100}, {110}, and {210} zones on the triangle and the locations of the directions common to more than one zone. (The hardnesses are listed in table I.)

To construct the stereographic representation, values from each curve were plotted along the appropriate zone of the triangle in the direction corresponding to the hardness value. The points with equal hardness values on the several zones were then connected by isohardness lines.

The stereographic representations of hardness anisotropy for the three BCC crystals examined are illustrated in figure 2. The hardness anisotropy behavior for all three crystals was similar. The hardness was at a maximum in the [001] direction. The minimum hardness is found in the [011] direction, with the [111] only slightly harder.

The W-3.2Re alloy was examined because of the lowering of the hardness of tungsten by the addition of rhenium up to approximately 5 percent observed by Pugh, Amra, and Hurd (ref. 7). Whether rhenium affects the hardness of tungsten alone, or also affects its hardness anisotropy can be readily determined from observation of the stereographic triangle. It is apparent that the effect of rhenium on the anisotropy of tungsten is small compared with the general decrease in hardness. The addition of rhenium, however, caused a slightly greater decrease in hardness in the [011] direction than in the [001].

The hardness anisotropy diagram for the FCC crystals is illustrated in figure 3. The anisotropy of aluminum is very similar to that shown by the BCC metals, with the maximum hardness in the [001] direction. The direction with the minimum hardness is not the [011], however, but the $[\bar{1}11]$.

The anisotropic behavior of the FCC crystal of LiF differs significantly from that shown by the cubic metals. In contrast to the cubic metals, the [001] direction in this ionic crystal exhibits the minimum hardness, and the [111] direction exhibits the greatest hardness. There is an additional hardness peak near the [011] direction.

The plane of indentation has a noticeable effect on the hardness anisotropy of CPH titanium. In the [0001] direction, common to the three prismatic planes listed in table II, the measured hardness values were similar. In the directions common to the basal and prismatic planes, however, differences in hardness were measured. The hardnesses measured on the prismatic planes were greater than those measured in the same direc-

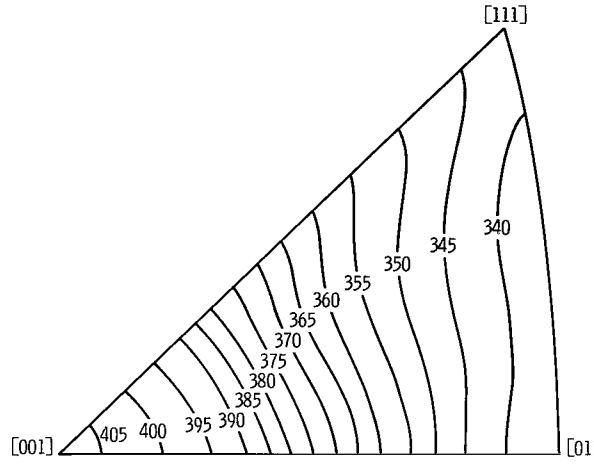

(a) Tungsten.

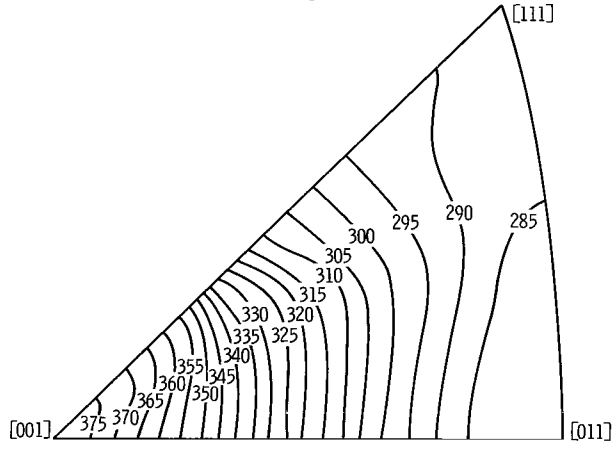

(b) Tungsten-3.2 percent rhenium.

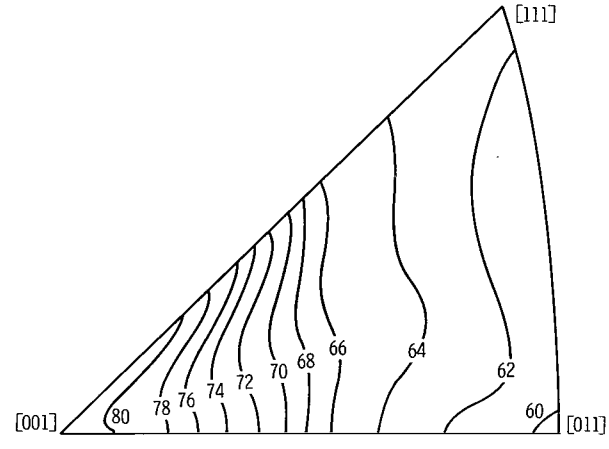

(c) Niobium.

Figure 2. - Stereographic representation of Knoop hardness anisotropy of body-centered-cubic crystals.

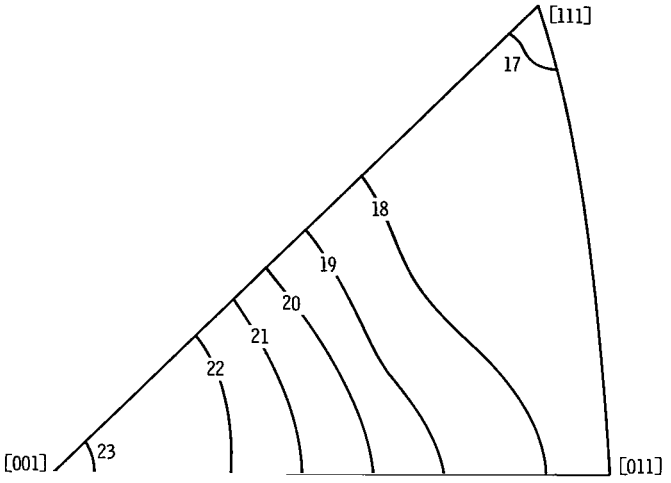

(a) Aluminum.

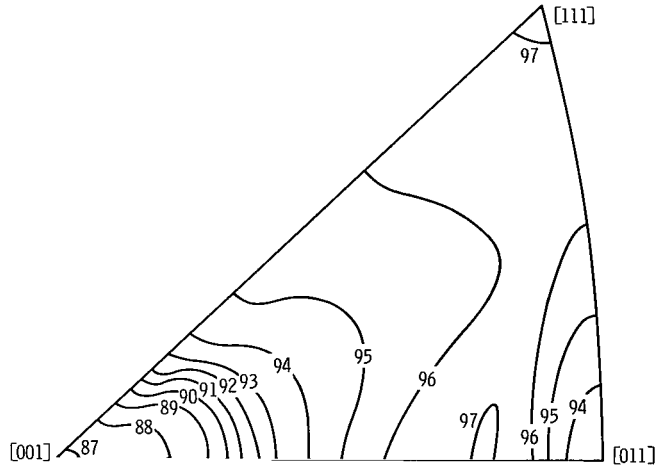

(b) Lithium fluoride.

Figure 3. - Stereographic representation of Knoop hardness anisotropy of face-centered-cubic crystals.

TABLE II. - KNOOP HARDNESS ANISOTROPY DATA FOR TITANIUM

Direction	Plane	Knoop hardness number	
		200-g load	Mean value
[0001]	$\{\bar{1}100\}$	36.7 ± 0.6	36.0
	$\{\bar{1}2\bar{1}0\}$	36.4 ± 0.6	
	$\{\bar{5}7\bar{2}0\}$	35.0 ± 1.3	
$\langle 10\bar{1}0\rangle$	(0001)	90.1 ± 2.7	101
	$\{\bar{1}2\bar{1}0\}$	111 ± 2.7	
$\langle 11\bar{2}0\rangle$	(0001)	99.1 ± 2.1	108
	$\{\bar{1}100\}$	117 ± 3.0	
$\langle 31\bar{4}0\rangle$	(0001)	97.3 ± 1.7	108
	$\{\bar{5}7\bar{2}0\}$	118 ± 2.7	

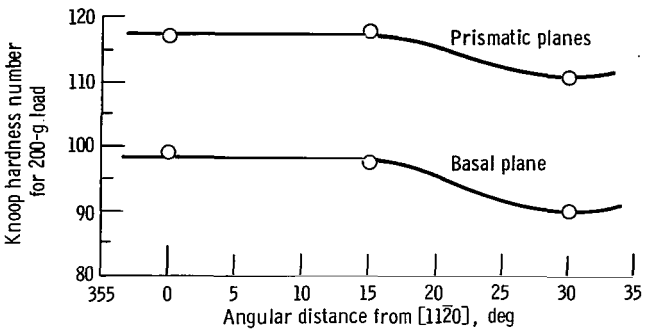

Figure 4. - Rotation of Knoop indentor on basal and prismatic planes of single-crystal titanium.

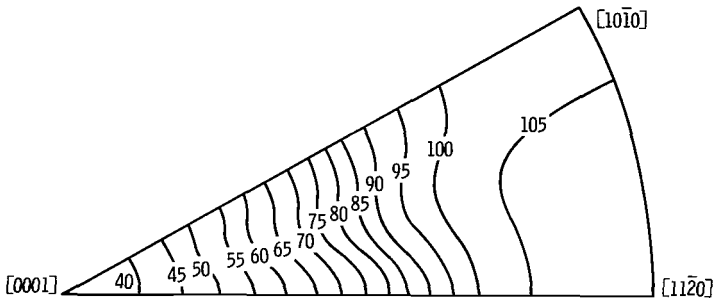

Figure 5. - Stereographic representation of Knoop hardness anisotropy of titanium crystal.

tions on the basal plane (fig. 4). The difference between the hardness values on the different planes is nearly constant, indicating that the effect of the plane is probably additive to the effect of direction on anisotropy. Because this difference is small compared with the almost threefold change in hardness with direction alone, the average values can be used in the stereographic diagram (fig. 5). Titanium exhibits a far greater hardness anisotropy than any of the cubic crystals.

DISCUSSION

The hardness anisotropy of the various crystals examined in this study was in general agreement with literature data. Both Douglass (ref. 2) and Daniels and Dunn (ref. 5) showed the same variation of hardness with indentor orientation on the {110} planes of niobium and silicon ferrite, respectively, as was seen in this study for the BCC metals. The greatest hardness was found in the ⟨100⟩ directions and the least in the ⟨110⟩.

Similarly, there is good agreement between the observed hardness anisotropy on both the {100} and {110} planes of aluminum and the literature data for aluminum (ref. 3)

and nickel (ref. 4). The maximum and minimum hardnesses were found in the $\langle 100 \rangle$ and $\langle 111 \rangle$ directions, respectively.

No data were found in the literature concerning the hardness anisotropy of ionic crystals.

Literature data describing the hardness anisotropy of the CPH metals are far less complete than for the cubic metals. The data are usually in the form of hardness values for specific directions on certain planes.

Feng and Elbaum (ref. 8) showed the same hardness variation for titanium on the prismatic plane as was found in this study. The hardness increased from the [0001] direction toward the $\langle 10\bar{1}0 \rangle$ direction. This finding is in contrast to the data of Daniels and Dunn (ref. 5) for zinc, where the maximum hardness was found in the [0001] direction. This apparent discrepancy can be partially resolved, however, by consideration of the anisotropy data compiled by Partridge and Roberts (ref. 9). These data indicate a correlation between the c/a ratio and the direction of maximum hardness. As the c/a ratio decreases through approximately 1.62, the direction of maximum hardness shifts from the [0001] to the $\langle 11\bar{2}0 \rangle$. The c/a ratios of zinc and titanium are 1.856 and 1.587, respectively, and thus, the anisotropy observed agrees with those observed by Partridge and Roberts.

The significance of the c/a ratio of 1.62 is not entirely clear. The proximity of this value to the ideal c/a ratio of 1.63 suggests that it is related to the density of atomic packing in the basal planes as compared with the prismatic planes.

The actual mechanism of deformation resulting in the observed hardness anisotropy is complicated by the complex stress state associated with indentor penetration. This complex stress state complicates any analysis of hardness anisotropy in terms of resolved shear stresses. The work of Daniels and Dunn (ref. 5) is the most comprehensive published analysis of shear stress data. Although many simplifying assumptions were made, their analysis apparently predicted the hardness anisotropy found for silicon ferrite, and was consistent with the hardness we found for other BCC metals. However, in an attempt to duplicate their analysis, we found that they neglected certain factors. When these factors are considered, the hardness variation predicted does not agree with their findings. Because this and other similar analyses have been accepted and used (refs. 2, 8, and 10), a summary and criticism of their analysis is presented.

In the model of Daniels and Dunn, hardness is treated as an inverse function of the ease of slip initiation. They assume that, for each indentor facet, the effective force causing deformation is a tensile force parallel to the steepest slope of the facet. For purposes of analysis, the deformation is considered to be that of small cylinders pulled in tension parallel to this effective force. From this model they derive an effective resolved shear stress which is directly proportional to the product of the cosines of three angles:

(1) between the slip direction and the effective force,

(2) between the normal-to-the-slip plane and the effective force,

(3) between the direction in the slip plane perpendicular to the slip direction and the direction in the indentor-facet plane perpendicular to the effective force.

For any slip system and indentor orientation these angles can be determined and an effective resolved shear stress calculated.

Computations based on their model for indentations on the {100} plane of a cubic metal, and for slip of the {112} ⟨111⟩ type result in the curves shown by the long-dashed lines of figure 6 (which is based on fig. 8 of ref. 5). Their curves show that the highest effective resolved shear stress, and therefore the easiest slip, is with the long axis of the indentor parallel to the ⟨110⟩ direction. As they predict, this easy slip corresponds to the lowest hardness, both for their silicon ferrite and for the BCC metals examined in this study. Similarly, the lowest effective resolved shear stress, at 45° from ⟨110⟩, corresponds to the highest hardness. However, in duplicating their results for this plane and slip system with the aid of a computer, not only were the curves they presented duplicated, but also, an additional curve resulted. This curve is shown in figure 6 by the solid line. Daniels and Dunn obviously failed to consider certain slip systems of the {112} ⟨111⟩ type. The full set of curves in figure 6 shows that the lowest effective resolved shear stress is near 30° from ⟨110⟩, not 45° as was found experimentally. Similar computations for indentions on the {100} plane involving the {110}⟨111⟩ and the {123}⟨111⟩ slip revealed similar results, indicating a discrepancy in their theoretical treatment.

Modifications of the Daniels and Dunn stress-state assumptions have been made in this study and by Feng and Elbaum (ref. 7). Instead of considering a tensile force parallel to the indentor facet as the effective deformation force, this force is, instead, a com-

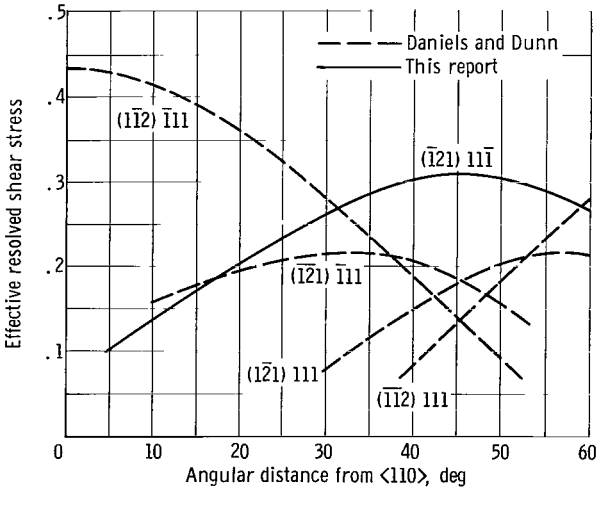

Figure 6. - Effective resolved shear stress as function of indentation orientation on (001) plane for slip on (112) planes.

pressive force which is perpendicular to the indentor facet. As in the case of the unmodified model, when all possible slip systems are considered, little agreement is found between the predicted hardness anisotropy and the experimental results. It is thus apparent that the theoretical description of hardness anisotropy by Daniels and Dunn is at variance with experimental observations.

An analysis of hardness anisotropy based on simple atomic packing on planes or in specific crystallographic directions cannot be supported by the data presented since both BCC and FCC metals have similar hardness anisotropy, but considerably different atomic packing.

CONCLUSIONS

As a result of this study on hardness anisotropy, the following conclusions were made:

1. The Knoop hardness anisotropy of several cubic materials is primarily a function of the crystallographic direction of the Knoop indentor, with the contribution of the plane of indentation relatively minor. With the hardness a function only of direction, it is therefore possible to represent the hardness anisotropy of a crystal on a standard stereographic triangle.

2. The hardness anisotropy of the body-centered-cubic and face-centered-cubic metals is similar, with the greatest hardness in the ⟨100⟩ directions. However, the directions of lowest hardness differ, being ⟨110⟩ for the body-centered-cubic metal structure and ⟨111⟩ for the face-centered-cubic metal structure.

3. Lithium fluoride, a cubic ionic crystal, in contrast to the cubic metals, showed the lowest hardness in the ⟨100⟩ direction.

4. Titanium, a close-packed hexagonal metal, showed a considerably greater anisotropy than any of the cubic metals. However, unlike the cubic crystals, the plane of indentation made a noticeable contribution to hardness anisotropy. The hardness along the c axis was considerably lower than that along the a axis, or along any other direction in the basal plane.

Lewis Research Center,
National Aeronautics and Space Administration,
Cleveland, Ohio, July 25, 1967,
129-03-02-05-22.

REFERENCES

1. French, David N.; and Thomas, David, A.: Hardness Anisotropy and Slip in WC Crystals. Trans. AIME, vol. 233, no. 5, May 1965, pp. 950-952.
2. Douglass, D. L.: Hardness Anisotropy of Columbium. Trans. ASM, vol. 54, 1961, pp. 322-330.
3. Petty, E. R.: The Hardness Anisotropy of Aluminum Single Crystals. J. Inst. Metals, vol. 91, 1962-63, pp. 54-62.
4. LaVecchia, A.; and Nicodemi, W.: Effect of Crystal Orientation on Microhardness of Nickel Single Crystals. Met. Ital., vol. 57, no. 9, Sept. 1965, pp. 321-326.
5. Daniels, F. W.; and Dunn, C. G.: The Effect of Orientation on Knoop Hardness of Single Crystals of Zinc and Silicon Ferrite. Trans. ASM, vol. 41, 1949, pp. 419-442.
6. Knoop, Frederick; Peters, Chauncey G.; and Emerson, Walter B.: A Sensitive Pyramidal-Diamond Tool for Indentation Measurements. J. Res. Natl. Bur. Std., vol. 23, no. 1, July 1939, pp. 39-61.
7. Pugh, J. W.; Amra, L. H.; and Hurd, D. T.: Properties of Tungsten-Rhenium Lamp Wire. Trans. ASM, vol. 55, 1962, pp. 451-461.
8. Feng, C.; and Elbaum, C.: Effect of Crystallographic Orientation and Oxygen Content of Knoop Hardness Values of Iodide Titanium. Trans. AIME, vol. 212, no. 1, Feb. 1958, pp. 47-50.
9. Partridge, P. G.; and Roberts, E.: The Microhardness Anisotropy of Magnesium and Zinc Single Crystals. J. Inst. Metals, vol. 92, 1963-64, pp. 50-55.
10. Schwartz, M.; Nash, S. K.; and Zeman, R.: Hardness Anisotropy in Single Crystal and Polycrystalline Magnesium. Trans. AIME, vol. 221, no. 3, June 1961, pp. 554-560.

"The aeronautical and space activities of the United States shall be conducted so as to contribute . . . to the expansion of human knowledge of phenomena in the atmosphere and space. The Administration shall provide for the widest practicable and appropriate dissemination of information concerning its activities and the results thereof."

—NATIONAL AERONAUTICS AND SPACE ACT OF 1958

NASA SCIENTIFIC AND TECHNICAL PUBLICATIONS

TECHNICAL REPORTS: Scientific and technical information considered important, complete, and a lasting contribution to existing knowledge.

TECHNICAL NOTES: Information less broad in scope but nevertheless of importance as a contribution to existing knowledge.

TECHNICAL MEMORANDUMS: Information receiving limited distribution because of preliminary data, security classification, or other reasons.

CONTRACTOR REPORTS: Scientific and technical information generated under a NASA contract or grant and considered an important contribution to existing knowledge.

TECHNICAL TRANSLATIONS: Information published in a foreign language considered to merit NASA distribution in English.

SPECIAL PUBLICATIONS: Information derived from or of value to NASA activities. Publications include conference proceedings, monographs, data compilations, handbooks, sourcebooks, and special bibliographies.

TECHNOLOGY UTILIZATION PUBLICATIONS: Information on technology used by NASA that may be of particular interest in commercial and other non-aerospace applications. Publications include Tech Briefs, Technology Utilization Reports and Notes, and Technology Surveys.

Details on the availability of these publications may be obtained from:

SCIENTIFIC AND TECHNICAL INFORMATION DIVISION

NATIONAL AERONAUTICS AND SPACE ADMINISTRATION

Washington, D.C. 20546